Optimization of Monocarboxylate Transporter 1 Blockers through Analysis and Modulation of Atropisomer Interconversion Properties

Simon D. Guile,[†,*] John R. Bantick,[†] Martin E. Cooper,[†,§] David K. Donald,[†] Christine Eyssade,[†] Anthony H. Ingall,[†] Richard J. Lewis,[‡] Barrie P. Martin,[†] Rukhsana T. Mohammed,[†] Timothy J. Potter,[‡] Rachel H. Reynolds,[†] Stephen A. St-Gallay,[‡] and Andrew D. Wright[‡]

Department of Medicinal Chemistry, AstraZeneca R&D Charnwood, Bakewell Road, Loughborough, LE11 5RH, UK, and Department of Physical & Metabolic Science, AstraZeneca R&D Charnwood, Bakewell Road, Loughborough, LE11 5RH, UK

Received August 17, 2006

We have previously described a novel series of potent blockers of the monocarboxylate transporter, MCT1, which show potent immunomodulatory activity in an assay measuring inhibition of PMA/ionomycin-induced human PBMC proliferation. However, the preferred compounds had the undesirable property of existing as a mixture of slowly interconverting rotational isomers. Here we show that variable temperature NMR is an effective method of monitoring how alteration to the nature of the amide substituent can modulate the rate of isomer exchange. This led to the design of compounds with increased rates of rotamer interconversion. Moreover, some of these compounds also showed improved potency and provided a route to further optimization.

Introduction

An important component of the immune response is activation of T cells following antigen challenge. However, undesirable activation can lead to graft rejection following transplantation and to autoimmune diseases such as rheumatoid arthritis.

We became interested in a report[1] describing a series of pyrrolopyrimidines as potential immunosuppressive agents. From this lead, following an extensive structural investigation, we identified a novel series of compounds exemplified by quinoline amide **1**.[2] Furthermore, through compound-led target identification[3] using photoaffinity labeling and proteomic characterization, we were able to show the previously unknown molecular target of these compounds to be the monocarboxylate transporter, MCT1. This was supported by a strong correlation between binding at MCT1 and *in vitro* immunomodulatory activity in an assay measuring inhibition of PMA/ionomycin-induced human PBMC proliferation.[4]

The monocarboxylate transporters are a family of proteins which transport lactate and other small monocarboxylates.[5] We have shown that MCT1 expression is rapidly upregulated upon T lymphocyte activation in order to meet the demand for lactate efflux resulting from an increased glycolytic rate. Inhibition of lactate efflux by potent blockade of lactate transport results in the accumulation of lactate within the cell and feedback inhibition of glycolysis. This suppression of cellular metabolism results in the inability of T lymphocytes to sustain the rapid rate of cell division occurring during the early immune response to antigen recognition, without being cytotoxic. Blockade of MCT1 is thus a novel mechanism of immunosuppression distinct from current therapies.

Quinoline amide **1** resulted from an optimization strategy which focused on reducing logD of highly potent but lipophilic leads. It was concluded that, in order to achieve a good balance of properties, assisted by maintaining low lipophilicity, such compounds require a heteroaryl group at the 6-position in combination with an amide group at the 5-position.[2] The preferred 5-amide was found to be the (*R*)-hydroxypyrrolidine amide. However, compounds containing this amide existed in solution as a mixture of atropisomers[6] (slowly equilibrating conformational isomers), due to restricted rotations at the amide (CO−N) and aryl−carbonyl (Ar−CO) bonds (Figure 1). For quinoline **1** and the closely related fluoro analogue **2**, we have been able to isolate, assign conformations, and, in the case of **2**, measure MCT1 potencies for each of the atropisomers.

Despite their good properties, progression of compounds such as **1** as potential drugs would be complicated by the existence of multiple conformational forms. These could present significant challenges due to potential safety, analytical, and manufacturing concerns.[7] There are numerous examples in the literature of atropisomers encountered during drug discovery programs.[8−13] Reports describe how atropisomerism has been simplified through symmetrization[9] or eliminated by making interconversion rapid.[10] Alternatively, restricting rotation has allowed isolation of a single conformer.[11,12]

To investigate the most suitable approach for our compounds, we prepared a range of amides with different electronic and steric properties. This led to an understanding of the factors affecting rates of conformer interconversion allowing the design of new amides which not only exhibited fast interconversion but also had other advantages over the previously preferred amides. We went on to make further modification resulting in highly optimized drug-like compounds.

Chemistry

While the synthesis of quinoline **1** has been previously described, the other target compounds **2**−**13** were prepared as shown in Schemes 1−4 below.

The N-1 isopropyl compounds **3** and **4** were prepared as shown in Scheme 1. The commercially available chloropyrimidinedione **14** was alkylated under forcing conditions with isopropyl iodide to give a mixture of the O-alkylated and desired N-alkylated products **15** and **16**, respectively. The substituted thiophene ring was incorporated in a three-step process to give the ester **17** which was then saponified to the acid **18**. Reaction

* Corresponding author: Tel: +44-1509-645308. Fax: +44-1509-645512. e-mail: simon.guile@astrazeneca.com.
† Department of Medicinal Chemistry.
‡ Department of Physical & Metabolic Science.
§ Current address: 7TM Pharma A/S, Fremtidsvej 3, 2970 Horsholm, Denmark.

10.1021/jm060995h CCC: $37.00
Published on Web 12/21/2006

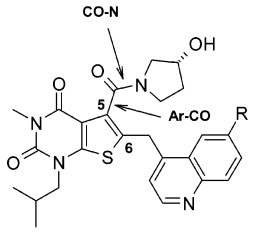

1: R = H
2: R = F

Figure 1. Compounds **1** and **2** with arrows indicating bonds with restricted rotation.

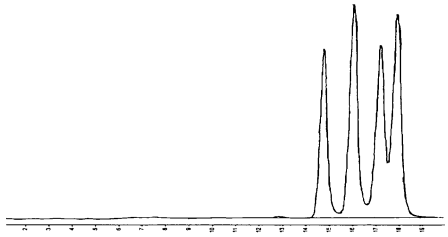

Figure 2. High-pressure liquid chromatogram (HPLC) of **2** showing the resolution of the atropisomeric forms (**2a**−**d**).

of the dianion derived from **18** with 2-trifluoromethylbenzaldehyde, followed by deoxygenation, provided the acid **19**. Conversion to the acid chloride followed by reaction with the appropriate amine gave amides **3** and **20**. The latter compound **20** was subsequently oxidized to the 1,3-thiazolidine dioxide **4**.

For compounds **5**, **8**, **11**, **12**, and **13** the intermediate esters **21c**−**g** were prepared from the previously described 6-methyl-5-ester **22**,[4] prepared analogously to **17**. Radical bromination provided key intermediate **23** which allowed introduction of the appropriate heterocycle. To prepare azetidine **5**, the ester **21c** was transformed directly to the amide followed by reaction with methylamine to derive the 6-substituent. The other esters were saponified to the acids **24d**−**g**. For targets **6**, **9**, and **10** the known acids **24a**,**b**[4] were prepared in a similar manner to **19**. Standard amide formation then gave the desired target compounds **6** and **8**−**13** (Scheme 2 and Table 5).

For fluoroquinoline **2**, the acid **25**[4] was first converted to the protected amide **26**. Incorporation of the quinoline gave **27** which, following deoxygenation and deprotection, provided **2** (Scheme 3). The 6-O-linked compound **7** was prepared from the 6-H compound **28**.[4] Chlorination provided the 6-chloro compound **29** which was displaced with naphthol giving **30**. Ester hydrolysis to give acid **31** followed by amide formation provided **7** (Scheme 4).

Results

(a) Structural Analysis of 1 and 2. For compounds containing the 5-(*R*)-hydroxypyrrolidine amide group (e.g., **1** and **2**), four atropisomers result from slow bond rotation since each bond can assume two orientations (s-cis and s-trans for the amide; axial-*R* and axial-*S* for the aryl-carbonyl). The four atropisomers can be observed by high-pressure liquid chromatography (HPLC) and NMR spectroscopy.

Rotation about the Ar−CO bond is restricted by a steric clash between the core heterocycle and the amide moiety and generates an axis of chirality in the molecule. Rotation about the amide bond is restricted for electronic reasons and generates configurational isomers.

Variable temperature NMR (VTNMR) on the fluoro quinoline **2** showed little line-broadening at 130 °C, suggesting very slow interconversion which was confirmed by the ability to separate the individual atropisomers by HPLC. These atropisomers could be individually analyzed by LC-NMR because of their relatively slow interconversion. The individual components were designated as **2a**, **2b**, **2c**, and **2d** in order of increasing HPLC retention times (Figure 2).

LC-NMR[14] analysis of **2** was performed and assignments of the individual atropisomers were made using standard methods (see Experimental Section). Assignments for **1** were made in a similar way, largely on a mixture of the four atropisomers and by reference to the assignments made for **2**. Confirmation that the elution order was the same for the atropisomers of **1** and **2** was made by NMR measurements on individual atropisomers isolated by analytical scale HPLC. The resonances obtained in this way for **1** and **2** are shown in Table 1. A comparison of the 1D proton spectra of the isolated atropisomers of **2** is shown in Figure 3.

Examination of the shifts in Table 1 and Figure 3 reveals interesting patterns in the data. For example, there are large differences in chemical shift about the pyrrolidine ring between equivalent protons in different atropisomers, and these differences can be as large as 1.4 ppm. There is also an interesting symmetry between 7α, 7*β* and 10α, 10*β*. In rotamers **a** and **b** the 10 protons are more deshielded than the 7 protons. This can be interpreted as an indication of the orientation about the amide bond caused by the expected anisotropic deshielding effect on protons syn to the carbonyl.[15] It is interesting to note a small (2 Hz) difference in the geminal proton coupling constants for the 7 protons dependent on the proposed orientation relative to the amide carbonyl. Related conformational effects of sp^2 systems two bonds distant from a methylene group have been described.[16] A significant symmetry is also noted when considering the *faces* of the pyrrolidine ring. Considering the pairs of geminal protons 7, 9, and 10, without exception, the α face is most deshielded in rotamers **a** and **c**. This suggests a deshielding influence of the 4-carbonyl and implies that **a** and **c** are related by rotation about both bonds. However, definitive proof of the conformational identity of the atropisomers was provided by a ROESY experiment on the equilibrium mixture. This showed specific ROE cross-peaks from 11 to one of 7α, 7*β*, 10α, and 10*β* for each atropisomer, thus leading directly to the conformation (Figure 4 and Table 2).

(b) Rate of Atropisomer Interconversion for 2a. **2a** was separated from the equilibrium mixture of **2** and re-equilibration was followed at 37 °C by LC-NMR. The rate of conversion of **2a** to **2d** predominated, followed by a slower conversion of **2a**/**2d** to **2b**/**2c** (Figure 5). Fitting first-order kinetics gave a rate constant for conversion of **2a** to **2d** (amide bond rotation), and an average value for conversion of **2a**+**2d** to **2b**+**2c** by either rotation of the Ar−CO bond or a concerted mechanism. Half-lives and activation energies at 37 °C were calculated as 60 min and 98 kJ/mol for rotation about the amide bond and 760 min and 105 kJ/mol for rotation about the Ar−CO bond (either with or without a concerted rotation of the amide bond).

(c) Mechanism of Interconversion. In the literature,[12b,17,18,19] there is much discussion as to whether atropisomer interconversion in related compounds proceeds via a concerted or sequential mechanism. The concerted mechanism implies that rotation about the carbonyl−aryl bond occurs most rapidly when accompanied by a simultaneous rotation about the amide bond. Such interdependence is referred to as geared or gated rotation and is understood in terms of steric clashes on Ar−CO bond rotation which are relieved by distortion (and concomitant

Scheme 1[a]

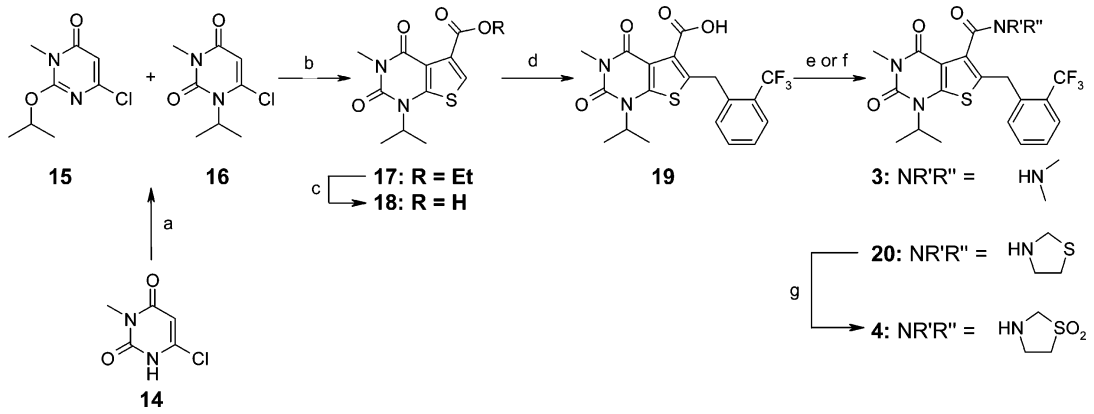

[a] Reagents and conditions: (a) iPrI, K_2CO_3, DMPU, 81% (3:4 O:N-alkylated); (b) (i) NaSH, EtOH; (ii) ethyl 3-bromopyruvate, H_2O; (iii) $TiCl_4$, DCM, 16% (three steps); (c) NaOH, H_2O, THF, MeOH, 95%; (d) (i) $CF_3C_6H_4CHO$, LDA, THF, −78 °C; ii) TFA, triethylsilane, 55% (two steps); (e) (i) oxalyl chloride, DMF (cat.), DCM; (ii) Me_2NH, Na_2CO_3, H_2O, 27% (two steps); (f) (i) oxalyl choride, DMF (cat.), DCM; (ii) thiazolidine, DCM; (g) mCPBA, DCM, 23% (three steps).

Scheme 2[a]

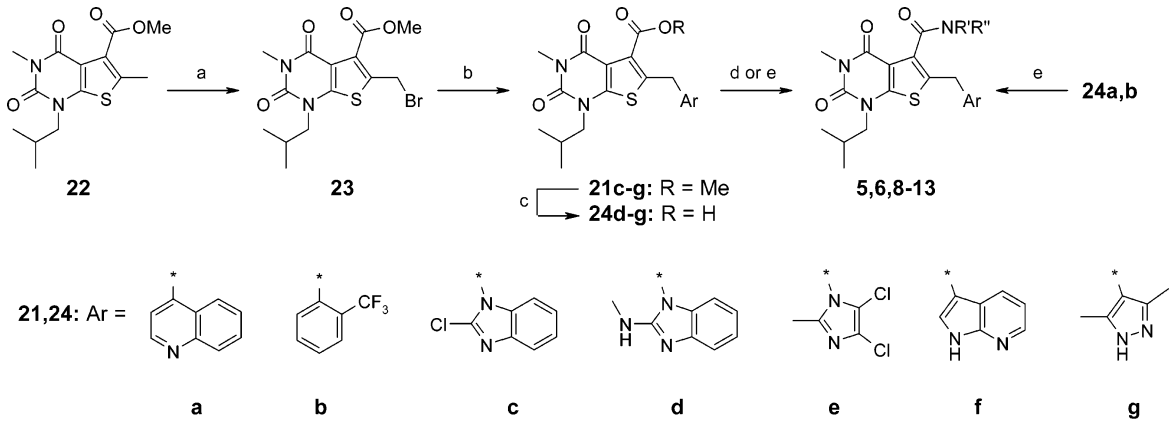

[a] Reagents and conditions: (a) NBS, chloroform, 76%; (b) 'imidazole', NaH, DMF 51−60% or azaindole, NaH, $ZnCl_2$, toluene, 49% or (i) zinc(II) acetylacetonate, DCM; (ii) hydrazine, DCM, 92% (two steps); (c) NaOH, H_2O, THF, MeOH, 76−92%; (d) (i) iPrMgCl, azetidine, THF, 28%; (ii) $MeNH_2$, H_2O, MeOH, THF, 130 °C, 38%; (e) RR′NH, EDCI, HOBt, DCM or (i) oxalyl choride, DMF (cat.), DCM; (ii) RR′NH, DCM; 16−81%.

Scheme 3[a]

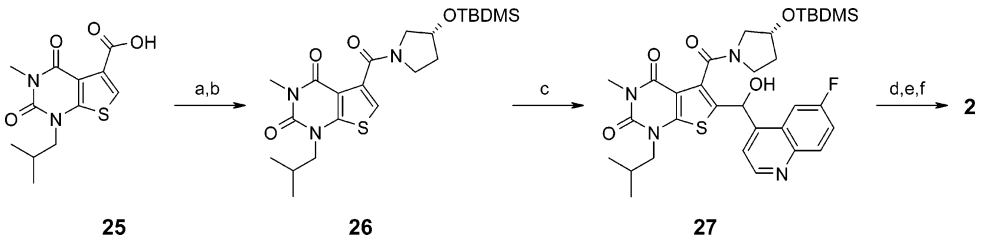

[a] Reagents and conditions: (a) (*R*)-3-hydroxypyrrolidine, EDCI, HOBt, DCM; (b) TBDMSCl, imidazole, DMF, 67% (two steps); (c) 6-fluoroquinoline-4-carbaldehyde, LDA, THF, −78 °C, 83%; (d) Ac_2O, TEA, DMAP, DCM; (e) H_2, Pd/C, $NaHCO_3$, H_2O, MeOH, EtOAc; (f) CH_3CN, HF(aq), 29% (three steps).

rotation) of the amide bond. In an attempt to determine how our compounds behaved, further kinetic measurements were carried out.

The individual atropisomers of **1** were separated by preparative HPLC and re-equilibration at 20 °C was followed by analytical HPLC. Modelmaker v4[20] was used to analyze the data (Figure 6). Although we were able to show similar rates of conversion of **1a** to **1d** and **1b** to **1c** by rotation about the amide bond, we were unable to determine whether rotation about the Ar−CO bond followed a concerted or nonconcerted mechanism. Due to the large difference in rates between rotation about the amide bond and the second process, adequate fits to the data could be obtained by allowing either mechanism or indeed both.

We note that our results show that amide bond rotation has the lowest energy, and the second process a somewhat higher energy (by 7 kJ/mol). This contrasts to the results of Johnston[17] and Albert[12b] who demonstrated that the concerted process was the lowest energy, but is similar to the results of Clayden,[18] though the difference in energy between the lowest energy process (amide bond rotation) and concerted bond rotation was found to be less.

(d) Potency Data for Separate Conformers. Following separation of the four atropisomers of **2** (**2a**−**d**) by preparative HPLC, the MCT1 potency of each conformer was measured over a 24 h time course at room temperature (Table 3). At all time points it can be seen that the most active conformer is **2c** followed by **2b** with the other conformers, **2a** and **2d**, being

Scheme 4[a]

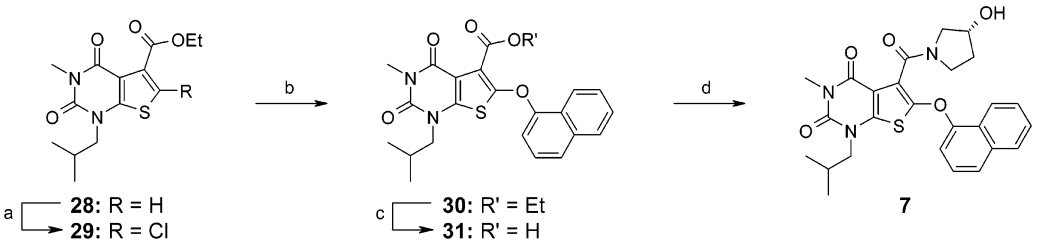

[a] Reagents and conditions: (a) NCS, HCl, DCM, 55%; (b) 1-naphthol, Cs_2CO_3, NMP, 54%; (c) NaOH, H_2O, THF, MeOH, 83%; (d) (*R*)-3-hydroxypyrrolidine, EDCI, HOBt, DCM, 31%.

Table 1. ^{1}H NMR Chemical Shifts of Pyrrolidine Resonances in Atropisomers of **1** and **2**. The α Face Is Defined as That Bearing the OH Group

pr ot on	1a	1b	1c	1d	2a	2b	2c	2d
7 α	*2.83 (dd, J = 11.2, 3.3 Hz)*	*2.96 (dt, J = 11.5, 1.6 Hz)*	*3.43 (dt, J = 13.1, 1.2 Hz)*	*3.48 (dt, J = 13.1, 1.6 Hz)*	*2.86 (dd, J = 11.5, 3.3 Hz)*	*2.92 (d, J = 11.5 Hz)*	*3.43 (d, J = 13.7 Hz)*	*3.41 (d, J = 13.3 Hz)*
7*β*	*2.47 (dd, J = 11.4, 5.4 Hz)*	*3.37 (dd, J = 11.7, 4.7 Hz)*	*3.29 (dd, J = 13.3, 4.9 Hz)*	3.72−3.76	*2.54 (dd, J = 11.5,5.0 Hz)*	*ca.* 3.30	*ca.* 3.30	*3.69 (dd, J = 13.3, 4.5 Hz)*
8*β*	*3.86 (qn, J = 4.5 Hz)*	4.40−4.42	4.24−4.26	4.53−4.55	*3.91 (qn, J = 4.3 Hz)*	4.38−4. 40	4.27−4. 30	4.49−4.52
9 α	1.78−1.85	1.95−2.01	1.61 (dddd, *J* = 12.9, 6.6, 3.4, 0.8 Hz)	1.75−1.80	1.80−1.85	1.93−1. 98	1.61−1. 65	1.72−1.77
9*β*	1.70−1.77	2.13−2.21	1.25−1.32	2.03 (dddd, *J* = 13.3, 9.2, 9.2, 4.7 Hz)	1.75−1.80	2.15−2. 20	1.30−1. 36	1.96−2.01
10 α	*3.59 (dt, J = 12.1, 7.8 Hz)*	3.63−3.67	3.10−3.18	3.08−3.14	*3.58 (dt, J = 12.1, 8.2 Hz)*	3.57−3. 62	3.10−3. 18	3.08−3.14
10 *β*	3.25−3.32	3.78−3.81	*2.39 (ddd, J = 10.7, 8.2, 2.3 Hz)*	3.24−3.27	*ca.* 3.30	3.74−3. 79	2.40−2. 46	3.23−3.28

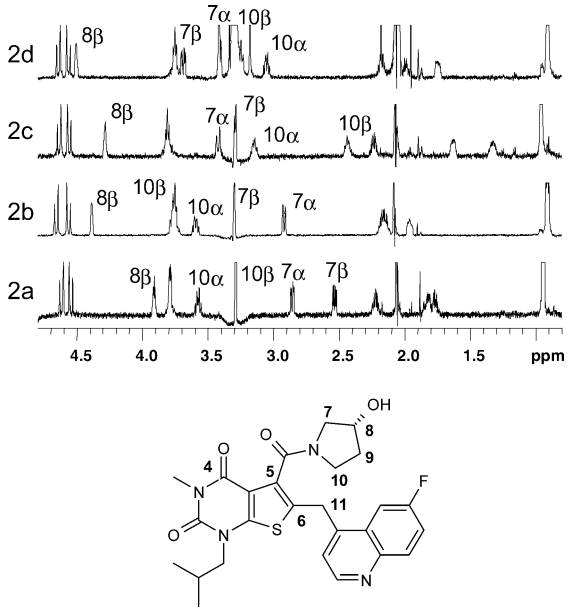

Figure 3. Partial LC-NMR spectra for the four atropsiomers of **2** indicating the large changes in chemical shift observed.

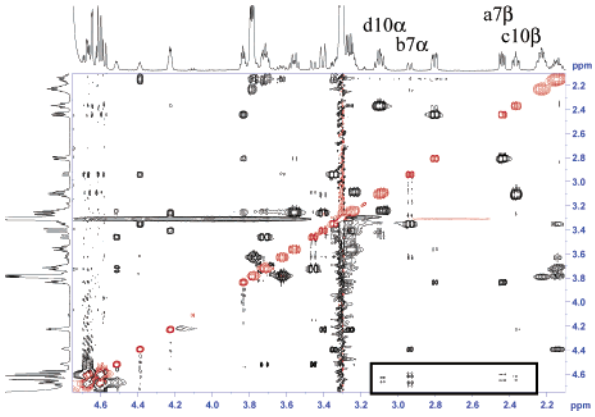

Figure 4. Partial ROESY spectrum for mixture of atropsiomers of **1** showing key ROE cross-peaks (boxed) between protons 11 and protons 7 and 10.

Table 2. ROE Cross-peaks Observed from **11** to the Pyrrolidine Protons and Deduced Conformation about the Amide and Ar−CO Bonds in Atropisomers of **1**

rotamer	ROE observed	conformation about amide bond	conformation about Ar−CO bond
1a	7*β*	trans	axial-*S*
1b	7α	trans	axial-*R*
1c	10*β*	cis	axial-*R*
1d	10α	cis	axial-*S*

less potent. Further interpretation is complicated by the fact that interconversion about the amide bond at room temperature occurs at a similar rate to the slow equilibration/slow on-rate kinetics of binding which is apparent from the data shown.

(e) Affecting Speed of Rotation. In order to avoid potential development issues arising from the atropisomeric nature of compounds such as **1** and **2**, alternative compounds were sought with the goal of accelerating bond rotation. With a target biological half-life of greater than 8 h we set as a criterion for conformer interconversion a half-life of less than 15 min.

We required a screen to rapidly evaluate the compounds for their atropisomeric properties, and variable temperature NMR was used for this purpose. Compounds were dissolved in DMSO-d_6 and NMR spectra obtained under automation at 25, 60, 90, and 130 °C. These spectra were examined, and coalescence temperature and rotamer signal separation were estimated. Using standard methods[21] it was then possible to *estimate* the half-life at 37 °C. Table 4 shows typical values obtained for a range of temperatures and signal separations using this methodology.

It is important to emphasize that the value of half-life obtained is only an estimate, of sufficient accuracy for us to rank compounds and assess structural changes. For example, no

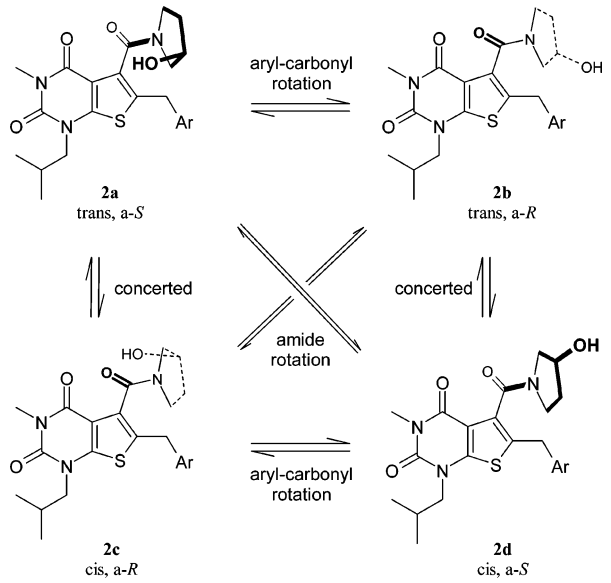

Figure 5. Structural assignments for atropisomers **2a**−**d**.

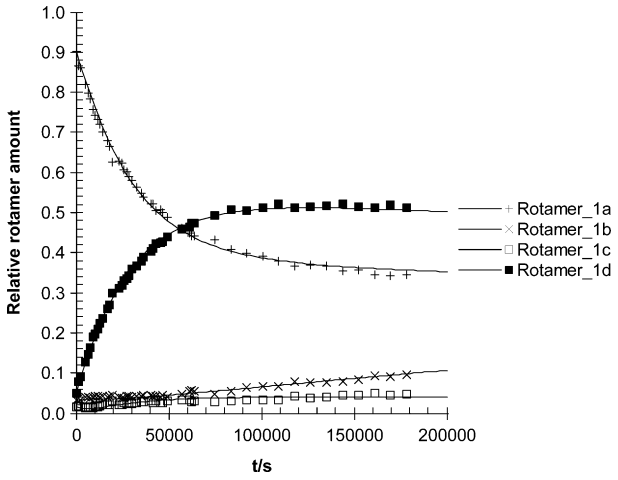

Figure 6. Fit of model to experimental data obtained for the room temperature interconversion of rotamers from **1a** start point.

Table 3. Potency Data for Separate Conformers[a]

compd	0.5 h	1 h	3 h	24 h
2	15	6.6	2.8	0.81
2a	489	507	172	18
2b	46	22	8.5	3.0
2c	13	4.9	1.7	0.66
2d	118	67	31	4.1

[a] SPA assay (nM).[2]

Table 4. Approximate Half-Life (in minutes) at 37 °C According to Rotamer Signal Separation and the Temperature (temp) at Which Coalescence Is Observed

temp, °C	2 Hz	5 Hz	20 Hz	50 Hz
∼150	∼110	∼30	∼5	∼1
110	2.5	0.8	0.1	5×10^{-2}
75	0.1	3×10^{-2}	7×10^{-3}	3×10^{-3}
<60	$<2 \times 10^{-2}$	$<8 \times 10^{-3}$	$<2 \times 10^{-3}$	$<7 \times 10^{-4}$

account has been made of the temperature dependence of $\Delta G^{\ddagger}$; coalescence temperatures and signal separations at coalescence are only estimates. We assume we can treat the two bond rotations independently and that rotamer populations are equal. In some cases it was not possible to distinguish two distinct coalescence processes, and a single half-life for both is given. While exploring numerous 5-amides, the heterocycle at the 6-position was also varied. It is assumed in this analysis that all methylene-linked (hetero)aryl groups at the 6-position have equal effect on rotation properties.

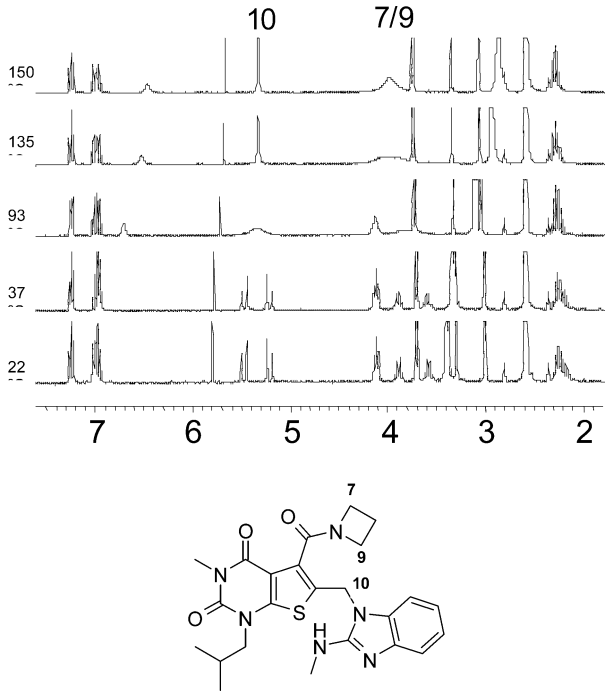

Figure 7. VTNMR of **5** showing different coalescence temperatures for rotation about the amide and Ar−CO bonds.

In order to validate the above approach, certain compounds were examined by VTNMR in greater detail, and one example, compound **5**, is shown in Figure 7. For this molecule, the methylene protons 10 are made diastereotopic by slow rotation about the Ar−CO bond below 93 °C. However, the azetidine protons (7 and 9) coalesce at 135 °C, indicating that for this compound the barrier to rotation about the amide bond is higher than that about the Ar−CO bond. Interestingly, for this compound, the pair of azetidine protons *on the same carbon* coalesce at virtually the same temperature as the methylene protons (they have a similar separation). From this simple observation we can deduce that the lower energy process is rotation about the Ar−CO bond only, i.e. it is definitely *not* a concerted rotation, which would coalesce protons on different carbons.

Using this VTNMR method to assess the rate of atropisomer interconversion, we examined a number of other 5-amides which had been prepared previously. In addition, in an effort to explain the effect of structural changes on interconversion rate, experimentally determined changes were compared with changes predicted by torsional driving calculations. While these molecular mechanics forcefields provide good estimates of steric hindrance, there is no explicit electronic consideration with all the amide bonds being treated equally. Therefore, any discrepancy between measured and calculated rates suggests a significant electronic influence.

The dimethyl amide **3** showed slow rotation as predicted, being no less sterically demanding than the pyrrolidine amide **2**. Both the sulfone **4** and the azetidine **5** amides showed considerably faster interconversion, and even the diol analogue **6** showed some increase in interconversion rate relative to the monohydroxy derivative **2**. For the azetidine example we rationalized this as a reduced steric clash from the azetidine ring in agreement with the modeling. For the sulfone and diol examples, reduced conjugation into the amide seemed the most

Table 5. Structures, Rotamer Interconversion Rates, and Properties of Compounds **1**−**13**[a]

Cmpd	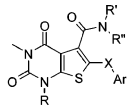			Amide t½ [b]	Ar-CO t½ [b,c]	MCT1 Binding K_i [d]	CYP2C9 IC_{50} [e]	CYP3A4 IC_{50} [e]	Rat Heps Cl_{int}	Hu Heps Cl_{int}	LogD
	R	NR'R"	XAr	min	min	nM	μM	μM	μL/min/10^6cells		
1	iBu			nd	nd	4.8	16	16	23	5.7	1.7
2	iBu			60±10	760±40	0.81	>50	>50	17	5.0	2.0
3	iPr			>30	>30	117	nd	nd	71	15	nd
4	iPr			~1	~1	>190	nd	nd	28	nd	2.6
5	iBu			0.15±0.1	0.006±0.004	59	8.9	1.0	3.0	<3	nd
6	iBu			~2	~2	29	nd	nd	24	1.0	1.2
7	iBu			~3	~3	0.31	4.7	7.2	65	73	2.9
8	iBu			~0.003 [f]	~3 [g]	3.2	15	44	8.7	3.2	2.3
9	iBu			~0.001	~0.001	0.52	13	46	24	5.6	2.2
10	iBu			nd	nd	0.09	0.83	8.3	44	nd	3.2
11	iBu			nd	nd	0.43	17	15	12	3.0	2.0
12	iBu			nd	nd	1.7	9.1	22	6.0	1.0	1.8
13	iBu			~0.0001 [f]	~0.002 [g]	1.2	23	100	5.3	<1	1.1

[a] nd = not determined. [b] Interconversion half-lives at 37 °C determined using the approximate VTNMR method (designated by > or ~ symbols) or using more accurate NMR measurements or other kinetic methods. [c] May be concerted in some cases. [d] SPA or filter binding assay.[2,4] The standard deviations for these assays were typically ±10% of mean. [e] The standard deviations for these assays were typically ±50% of mean. [f] Assumed to be amide bond rotation. [g] Assumed to be Ar−CO bond rotation.

likely cause for increased interconversion rate. While conformational effects resulting in reduced steric interactions could be an alternative explanation, this is not supported by the modeling. Although the latter three compounds had appreciably increased rotation rates, none had suitable potency for progression (Table 5).

An alternative approach to fast interconversion was to replace the 6-methylene linking group with a heteroatom. In the ether **7**, it was expected that the oxygen link would provide less steric encumbrance to rotation and would also benefit electronically in stabilizing the steric rotation transition state through resonance (vinylogous carbamate). Rapid rotation was indeed observed but further compounds of this type were not pursued, for while **7** had excellent activity at MCT1, its high logD resulted in poor *in vitro* metabolic stability and high human plasma protein binding (>99% bound). Attempts to combine the oxygen link with a suitable heterocycle were unsuccessful.

Returning to alternative amides, we speculated that an alkoxyamide would have the desired properties for rapid interconversion. The first example of this type to be prepared

was the 'Weinreb amide' **8**.[22] The structure of this alkoxyamide **8** was determined by single-crystal X-ray diffraction (see Supporting Information), and this was used as a basis for the modeling work described here. This structural modification had a profound positive effect on rotation rate, reducing the barriers to rotation about both the amide and Ar−CO bonds. Although one explanantion for this effect could be reduced conjugation in the amide bond resulting in more rapid rotation about both restricted bonds, we rationalized this effect as being due to reduced steric demand resulting from switching a methylene unit to oxygen. The latter hypothesis was supported by modeling data. Importantly, this rapidly interconverting compound **8** had potency and other properties comparable with the atropisomeric lead **1**.

Combining features of the alkoxyamide motif with the previously optimized (*R*)-hydroxypyrrolidine gave the (*S*)-hydroxyisoxazolidine **9** which, as well as a suitable, fast rotation rate, also showed excellent potency. Despite the higher logD of (*S*)-hydroxyisoxazolidine **9** relative to (*R*)-hydroxypyrrolidine **1**, both metabolic stability and CYP inhibition were at least as good.

(f) Optimization of Hydroxyisoxazolidine-Containing Compounds. Having found a nonatropisomeric amide with good properties, further optimization was investigated. Initially, the (*S*)-hydroxyisoxazolidine amide was combined with a range of previously explored 6-arylmethyl groups and gave similar SAR.[2] For example, 6-trifluoromethylbenzyl compound **10** was more potent than the quinoline analogue **9** but also showed higher CYP2C9 inhibition and lower metabolic stability. The azaindole **11** and methylaminobenzimidazole **12** containing derivatives were similar in properties to quinoline **9**, having slightly improved metabolic stability.

Continuing with the strategy of lowering lipophilicity and encouraged by the properties of monocyclic heterocycle **8**, further monoheterocyclic 6-substituents were explored. This work resulted in the discovery of the dimethylpyrazole **13**. This compound is better than the starting compound **1** in each of the properties indicated in Table 5. Besides having no atropisomer issue, compound **13** exhibits excellent potency and metabolic stability as well as low CYP inhibition. In addition, **13** is more soluble than 1 (2.9 mg/mL vs 0.5 mg/mL, respectively).

Summary

Rapid VTNMR methods have been used to guide the synthesis of nonatropisomeric MCT1 blockers. Combining potency conferring, rapidly interconverting amides with further logD lowering modifications has culminated in the identification of potent MCT1 blockers, exemplified by pyrazole **13**, possessing good drug-like properties.

A more detailed study of compounds **1**, **2**, and **5** has shown that the fastest interconversion in each case, amide rotation for the former two compounds and Ar−CO bond rotation for the latter, proceeds without concerted rotation of the other bond. This contrasts with some other literature reports. It is therefore likely that the mechanism of atropisomer interconversion, i.e., whether concerted or not, is highly dependent on the exact nature of substituents present on the compounds being studied.

Experimental Section

LC-NMR Separation and Analysis of 2. LC-NMR analysis of **2** was performed on a 600 MHz Varian Unity Inova Spectrometer (Palo Alto) fitted with an HPLC-NMR system comprising a Varian 9012 pump, 9050 UV detector, and HPLC-NMR Analyte Collector (Palo Alto, CA). A Jones Chromatography 7600 series solvent degasser and 7971 Column Heater (Lakewood, CA) were also used. The flow probe had a total volume of 110 μL and active volume of 60 μL. Data were collected on the peaks of interest using the stopped-flow method and the WET method[23] to suppress the resonances from residual methanol and protonated water. Suppression was achieved using "seduce" pulses of approximately 20 ms duration. Separation of the atropisomers of **2** was carried out using a Kromasil column (3.2 × 250 mm, 5 μm packing) and using an isocratic method (60% CD_3OD, 40% D_2O, 0.025% ammonium acetate), 0.5 mL/min, 20 °C. Peak detection was by UV at 280 nm.

Proton spectra were acquired on each separated atropisomer (Figure 3), and COSY and ROESY spectra on selected isomers. Assignment of the pyrrolidine protons to the α or β face was made on the basis of ROE cross-peaks and coupling constants. ROESY and eCOSY spectra were also acquired on an equilibrium mixture of the atropisomers. These spectra enabled additional coupling constants around the pyrrolidine ring to be measured, and the assignment of the atropisomers to conformations about the amide and Ar−CO bonds to be made.

Kinetics Measurements of 2. Atropisomer **2a** was collected in the NMR flow cell and equilibrated at 37 °C over 60 h. Integrating NMR resonances in the aromatic region allowed the rate of appearance of **2d** to be followed (rotation about the amide bond). The rate of appearance of **2b**+**2c** (from **2a**+**2d**) was taken as representing rotation about the Ar−CO bond. As peaks for **2a** and **2c** were coincident, the amount of **2c** present was estimated as being the same as the amount of **2b** (which could be integrated). The rate of appearance of **2d** and rates of appearance of **2b**+**2c** were fitted to an expression for reversible reaction kinetics, with the rate of approach to equilibrium (k_1+k_{-1}) as the rate constant. This simplified and approximate approach gave a reasonable fit (R^2 = 74%, $t_{1/2}$ = 60 min ± 10 min) for rotation about the amide bond, and a good fit (R^2 = 95%, $t_{1/2}$ = 12.7 h ± 0.6 h) for rotation about the Ar−CO bond.

Kinetic Measurements and Atropisomer Identification of 1. The atropisomers of **1** were isolated by HPLC on an Agilent 1100 series purification system using a Kromasil column (3.2 × 250 mm, 5 μm packing) and an isocratic method (60% CH_3OH, 40% H_2O, 0.025% ammonium acetate), 0.5 mL/min, 20 °C. Peak detection was by UV at 280 nm. The kinetics of rotamer interconversion were followed at 20 °C by HPLC using the same chromatographic conditions; data was obtained from each of the four rotamer startpoints. ROESY and eCOSY spectra were acquired on an equilibrium mixture of **1** in 60% CD_3OD, 40% D_2O on a Bruker Avance 600 MHz spectrometer. This confirmed that the assignments for **1** were very similar to **2**. Fractions of each atropisomer were collected, and a portion of each was dried. Proton NMR spectra were acquired, and this confirmed that the elution order for rotamers of **1** and **2** were identical.

Variable Temperature NMR. Variable temperature NMR was performed on a Varian UnityInova spectrometer at 300 or 400 MHz, usually under automation. Spectra at the different temperatures were assessed as described in the text.

Chemistry. Reagents were obtained from Aldrich Chemical or Lancaster Chemical companies and used without purification. High-performance liquid chromatography (HPLC) grade solvents were obtained from Fisher Scientific. Unless otherwise stated, reactions were carried out at ambient temperature (18−25 °C) and under positive nitrogen pressure with magnetic stirring. TLC was performed on Merck silica gel 60 F254 plates and visualized under UV light (254 nm) or by staining with potassium permanganate ($KMnO_4$). Flash chromatography was performed on E. Merck 230−400 mesh silica gel 60. Preparative reverse phase (RP)HPLC separations were performed using a Waters Symmetry, Novapak, or Xterra column. Routine NMR spectra were recorded on a Varian Unity spectrometer at a proton frequency of either 300 or 400 MHz. Chemical shifts are expressed in ppm relative to TMS (^{1}H, 0 ppm) or $CDCl_3$ (^{13}C, 77.0 ppm); coupling constants are expressed in Hz. Mass spectra were measured on either a VG 70-250S spectrometer using electron impact ionization (EI) or on an Agilent 1100 MSD G1946D spectrometer using electrospray ionization (ESI) or

atmospheric pressure chemical ionization (APCI); generally only ions which indicate the parent mass are reported.

6-[(6-Fluoroquinolin-4-yl)methyl]-5-{[(3*R*)-3-hydroxypyrrolidin-1-yl]carbonyl}-1-isobutyl-3-methylthieno[2,3-*d*]pyrimidine-2,4(1*H*,3*H*)-dione (2). Acetic anhydride (0.13 mL, 1.3 mmol) was added to a solution of compound **27** (0.57 g, 0.88 mmol), triethylamine (0.25 mL, 1.8 mmol), and DMAP (0.01 g, 0.08 mmol) in dichloromethane (5 mL) and the mixture stirred for 30 min. The mixture was concentrated under reduced pressure. Methanol (5 mL), ethyl acetate (2 mL), and saturated aqueous sodium bicarbonate solution (1.2 mL) were added followed by 10% palladium on charcoal (100 mg), and the mixture was stirred under hydrogen at 5 atm for 20 h. The reaction mixture was filtered through Celite and concentrated under reduced pressure. The residue was dissolved in acetonitrile (10 mL) and treated with 40% hydrofluoric acid (0.5 mL). After 18 h, the mixture was poured into saturated aqueous sodium bicarbonate solution (50 mL) and extracted with ethyl acetate (3 × 50 mL), dried ($MgSO_4$), and concentrated under reduced pressure. The residue was purified by flash chromatography (elution with 14:1 dichloromethane:ethanol) and further by RPHPLC to give compound **2** as a colorless foam (0.13 g, 29%). ^{1}H NMR (300 MHz, DMSO-d_6): δ 8.86−8.83 (m, 1H), 8.18−8.09 and 8.02 (m, 2H), 8.04 (d, J = 8.0 Hz, 1H), 7.70 (td, J = 8.7, 2.8 Hz, 1H), 7.55−7.45 (m, 1H), 5.02 and 4.99 and 4.93 and 4.85 (4 × d, 1H), 4.58−4.43 (m, 2H), 4.37−4.18 (m, 2H), 3.70−3.60 (m, 2H), 3.60−3.08 (m, 1H), 3.20 (s, 3H), 2.95−2.68 (m, 1H), 2.19−2.06 (m, 1H), 2.00−1.64 (m, 2H), 0.93−0.81 (m, 6H), complex due to atropisomerism (see text for assignment of individual rotamers). APCI-MS *m*/*z*: (pos) 511 [M + H]$^+$. Anal. ($C_{26}H_{27}FN_4O_4S$. H_2O) H, N; C: calcd, 58.98; found, 59.40; S calcd, 6.05; found, 5.58.

1-Isopropyl-*N*,*N*,3-trimethyl-2,4-dioxo-6-[2-(trifluoromethyl)-benzyl]-1,2,3,4-tetrahydrothieno[2,3-*d*]pyrimidine-5-carboxamide (3). Oxalyl chloride (0.73 mL, 8.4 mmol) followed by DMF (2 drops) was added to compound **19** (1.2 g, 2.8 mmol) dissolved in dichloromethane (30 mL). The reaction mixture was stirred for 90 min and then concentrated under reduced pressure. The residue was dissolved in tetrahydrofuran (24 mL), and an aliquot (2 mL) of this solution was added to dimethylamine (40% aq; 0.13 mL, 0.17 mmol) in a saturated solution of sodium carbonate (10 mL). The reaction mixture was stirred for 2 h and then extracted with dichloromethane providing compound **3** as a colorless solid (28 mg, 27%). ^{1}H NMR (300 MHz, $CDCl_3$): δ 7.67 (d, J= 6.0 Hz, 1H), 7.56−7.49 (m, 2H), 7.40−7.35 (t, J=7.4 Hz, 1H), 4.5 (br s, 1H), 4.25 (d, J= 16.0 Hz, 1H), 4.17 (d, J= 16.0 Hz, 1H), 3.36 (s, 3H), 3.15 (s, 3H), 2.87 (s, 3H), 1.56−1.52 (m, 6H); APCI-MS *m*/*z*: (pos) 454 [M + H]$^+$. Anal. ($C_{21}H_{22}F_3N_3O_3S$) H, N, S; C calcd, 55.62; found, 56.28.

5-[(1,1-Dioxido-1,3-thiazolidin-3-yl)carbonyl]-1-isopropyl-3-methyl-6-[2-(trifluoromethyl)benzyl]thieno[2,3-*d*]pyrimidine-2,4(1*H*,3*H*)-dione (4). mCPBA (70−75%: 0.5 g, 2.2 mmol) was added to crude compound **20** (0.15 g, 0.3 mmol) in dichloromethane (5 mL) and stirred at room temperature for 24 h. The reaction mixture was washed with 10% sodium metabisulfite solution, dried ($MgSO_4$), and concentrated under reduced pressure to give a brown oil which was purified by flash chromatography (elution with 4:6 ethyl acetate:*iso*-hexane). Recrystallization from ethyl acetate:*iso*-hexane gave **4** as a colorless solid (37 mg, 23%). mp. 194.4−195.6 °C. ^{1}H NMR (300 MHz, $CDCl_3$): δ 7.69 (d, J= 9.0 Hz, 1H), 7.55−7.4 (m, 3H), 4.74 and 4.61(d, J= 12.0 Hz, 1H), 4.5−4.14 (m, 5H), 3.92−3.88 + 3.67−3.6 (m, 1H), 3.46−3.05 (m, 5H), 1.57−1.53 (m, 6H); ESI-MS *m*/*z*: (pos) 530 [M + H]$^+$. Anal. ($C_{22}H_{22}F_3N_3O_5S_2$) C, H, N; S calcd, 12.11; found, 11.16.

5-(Azetidin-1-ylcarbonyl)-1-isobutyl-3-methyl-6-{[2-(methylamino)-1*H*-benzimidazol-1-yl]methyl}thieno[2,3-*d*]pyrimidine-2,4(1*H*,3*H*)-dione (5). Isopropylmagnesium chloride (2 M in ether; 0.25 mL, 0.43 mmol) was added to azetidine (0.03 mL, 0.43 mmol) in tetrahydrofuran. After 15 min, compound **21c** (0.20 g, 0.43 mmol) was added dropwise to the mixture. After 15 min further, azetidine (0.03 mL, 1.29 mmol) and isopropylmagnesium chloride (2 M in ether; 0.75 mL, 1.29 mmol) were added. After 15 min, the reaction mixture was quenched with water and then extracted with ethyl acetate. The organic layer was dried ($MgSO_4$), concentrated under reduced pressure, and purified by flash chromatography. A mixture of this compound and methylamine (2 M in THF, 0.6 mL, 1.2 mmol) in ethanol (6 mL) was heated in a pressurized vessel at 130 °C for 24 h. The reaction mixture was concentrated under reduced pressure. The residue was purified by silica chromatography (elution with 2% methanol in dichloromethane). The product obtained was recrystallized from dichloromethane:*iso*-hexane to give compound **5** as a colorless solid (0.023 g, 38%). mp: 276−276.5 °C. ^{1}H NMR (300 MHz, $CDCl_3$): δ 7.49 (1H, d, J = 6.0 Hz), 7.17−7.07 (3H, m), 6.75(1H, m), 5.3 (1H, s), 5.14 (1H, s), 4.3 (1H, m), 4.3−4.1 (2H, m), 3.8−3.7 (2H, m),3.6 (1H, m), 3.41 (3H, s), 3.07 (3H, d, J = 3.0 Hz), 2.3 (2H, m), 2.2 (1H, m), 0.92 (6H, d, J = 9.0 Hz). APCI-MS *m*/*z*: (pos) 481 [M + H]$^+$. Anal. ($C_{24}H_{28}N_6O_3S$·0.8CH_2Cl_2) C, H, N, S.

5-{[(3*R*,4*S*)-3,4-Dihydroxypyrrolidin-1-yl]carbonyl}-1-isobutyl-3-methyl-6-(quinolin-4-ylmethyl)thieno[2,3-*d*]pyrimidine-2,4-(1*H*,3*H*)-dione (6). To a suspension of compound **24a**[4] (200 mg, 0.45 mmol) in dichloromethane (3 mL) was added 1-hydroxybenzotriazole hydrate (120 mg, 0.89 mmol), and the mixture was stirred for 15 min. 1-Ethyl-3-(3′-dimethylaminopropyl)carbodiimide hydrochloride (171 mg, 0.89 mmol) was then added and stirring continued for 30 min. (3*R*,4*S*)-Pyrrolidine-3,4-diol[24] (125 mg, 0.90 mmol) was added, and the mixture was stirred for a further 3 h. The mixture was poured into saturated sodium bicarbonate solution (100 mL) and extracted with ethyl acetate, dried ($MgSO_4$), and concentrated under reduced pressure. The residue was purified by flash chromatography (elution with 1:3 ethanol:dichloromethane). The residue was further purified by RPHPLC to give compound **6** as a colorless solid (40 mg, 16%). mp: ∼120 °C. ^{1}H NMR (400 MHz, DMSO-d_6): δ 8.86 (d, J = 4.0 Hz, 1H), 8.27 and 8.22 (d, J = 8.0 Hz, 1H), 8.04 (d, J = 8.0 Hz, 1H), 7.77 (t, J = 8.0 Hz, 1H), 7.68−7.62 (m, 1H), 7.48 and 7.42 (d, J = 4.0 Hz, 1H), 5.02 and 4.99 and 4.85 and 4.75 (br s, 2H), 4.49 (br s, 2H), 4.10−3.90 (m, 2H), 3.68−3.60 (m, 3H), 3.48−3.36 (m, 1H), 3.20 (s, 3H), 3.02−2.98 (m, 1H), 2.95−2.92 and 2.82−2.78 (m, 1H), 2.12 (nonet, J = 7.0 Hz, 1H), 0.88−0.81 (m, 6H) - complex due to atropisomerism. APCI-MS *m*/*z*: (pos) 509 [M + H]$^+$. Anal. ($C_{26}H_{28}N_4O_5S$·2.2H_2O) C, H; N: calcd, 10.21; found, 11.70; S calcd, 5.83; found, 4.61.

5-{[(3*R*)-3-Hydroxypyrrolidin-1-yl]carbonyl}-1-isobutyl-3-methyl-6-(1-naphthyloxy)thieno[2,3-*d*]pyrimidine-2,4(1*H*,3*H*)-dione (7). Prepared using the same method as for **6** but employing acid **31** and (*R*)-3-hydroxypyrrolidine (colorless solid, 0.06 g, 31% yield). mp: 165−172 °C. ^{1}H−NMR (300 MHz, 130 °C, DMSO-d_6): δ 8.22−8.15 (m, 1H), 7.98−7.92 (m, 1H), 7.74 (d, J = 8.3 Hz, 1H), 7.61−7.55 (m, 2H), 7.49−7.44 (m, 1H), 7.30 (d, J = 7.7 Hz, 1H), 4.50−4.12 (m, 2H), 3.67 (d, J = 7.5 Hz, 2H), 3.60−3.05 (m, 4H), 3.25 (s, 3H), 2.27−2.11 (m, 1H), 2.08−1.66 (m, 2H), 0.90 (d, J = 6.7 Hz, 6H). APCI-MS *m*/*z*: (pos) 494 [M + H]$^+$. Anal. ($C_{26}H_{27}N_3O_5S$) C, H, N, S.

6-[(4,5-Dichloro-2-methyl-1*H*-imidazol-1-yl)methyl]-1-isobutyl-*N*-methoxy-*N*,3-dimethyl-2,4-dioxo-1,2,3,4-tetrahydrothieno-[2,3-*d*]pyrimidine-5-carboxa mide (8). Prepared using the same method as for **3** but employing acid **24e** and dimethylhydroxylamine hydrochloride (colorless solid, 8.18 g, 79% yield). mp: 138−140 °C. ^{1}H NMR (300 MHz, $CDCl_3$): δ 5.23 (s, 2H), 3.72 (d, J = 7.0 Hz, 2H), 3.55 (s, 3H), 3.23 (s, 3H), 3.16 (s, 3H), 2.32 (s, 3H), 2.21 (nonet, J = 7.0 Hz, 1H), 0.92 d, J = 7.0 Hz, 6H). APCI-MS *m*/*z*: (pos) 488/490/492 [M + H]$^+$. Anal. ($C_{19}H_{23}Cl_2N_5O_4S$) C, H, N, S.

5-{[(4*S*)-4-Hydroxyisoxazolidin-2-yl]carbonyl}-1-isobutyl-3-methyl-6-(quinolin-4-ylmethyl)thieno[2,3-*d*]pyrimidine-2,4(1*H*,3*H*)-dione (9). Prepared using the same method as for **6** but employing acid **24a** and (*S*)-4-isoxazolidinol hydrochloride[25] (colorless solid, 0.90 g, 81% yield). mp: 127−137 °C. ^{1}H NMR (300 MHz, DMSO-d_6): δ 8.86 (d, J = 5.0 Hz, 1H), 8.24 (d, J = 7.0 Hz, 1H), 8.05 (d, J = 7.0 Hz, 1H), 7.78 (t, J = 7.0 Hz, 1H), 7.63 (t, J = 7.0 Hz, 1H), 7.46 (d, J = 5.0 Hz, 1H), 5.54 (d, J = 5.0 Hz, 1H), 4.79 (d, J = 5.0 Hz, 1H), 4.67−4.52 (m, 2H), 4.11−4.03 (m, 1H), 3.95−3.89 (m, 1H), 3.82−3.80 (m, 1H), 3.67−3.54 (m, 3H),

3.21 (s, 3H), 2.08 (nonet, $J = 6.8$ Hz, 1H), 0.87 (d, $J = 6.5$ Hz, 6H). APCI-MS *m/z*: (pos) 495 $[M + H]^+$. Anal. ($C_{25}H_{26}N_4O_5S$) C, H, N, S.

5-[(4*S*)-4-Hydroxy-2-isoxazolidinylcarbonyl]-3-methyl-1-(isobutyl)-6-[2-(trifluoromethyl)phenylmethyl]-thieno[2,3-*d*]pyrimidine-2,4(1*H*,3*H*)-dione (10). Prepared using the same method as for **6** but employing acid **24b** and (*S*)-4-isoxazolidinol hydrochloride[25] (colorless solid, 1.66 g, 70% yield). mp: 127−131 °C. ^{1}H NMR (300 MHz, DMSO-d_6): δ 7.75 (d, $J = 7.5$ Hz, 1H), 7.69−7.62 (m, 1H), 7.53−7.45 (m, 2H), 5.53−5.48 (m, 1H), 4.80−4.59 (m, 1H), 4.26−4.16 (m, 2H), 3.79−3.47 (m, 6H), 3.22 (s, 3H), 2.11 (quintet, $J = 6.8$ Hz, 1H), 0.87 (d, $J = 6.5$ Hz, 6H). APCI-MS *m/z*: (pos) 512 $[M + H]^+$. Anal. ($C_{23}H_{24}F_3N_3O_5S$) C, H, N.

5-{[(4*S*)-4-Hydroxyisoxazolidin-2-yl]carbonyl}-1-isobutyl-3-methyl-6-(1*H*-pyrrolo[2,3-*b*]pyridin-3-ylmethyl)thieno[2,3-*d*]pyrimidine-2,4(1*H*,3*H*)-dione (11). Prepared using the same method as for **6** but employing acid **24f** and (*S*)-4-isoxazolidinol hydrochloride[25] (colorless solid, 0.06 g, 31% yield). mp: 159−161 °C. ^{1}H NMR (300 MHz, DMSO-d_6): δ 11.53 (br s, 1H), 8.20−8.18 (m, 1H), 7.97−7.90 (m, 1H), 7.44−7.41 (m, 1H), 7.02−6.99 (m, 1H), 5.55−5.50 (m, 1H), 4.80−4.60 (m, 1H), 4.18−4.00 (m, 3H), 3.90−3.75 (m, 2H), 3.68−3.53 (s, 3H), 3.21−3.20 (m, 3H), 2.13−2.03 (m, 1H), 0.85−0.82 (m, 6H). APCI-MS *m/z*: (pos) 484 $[M + H]^+$. Anal. ($C_{23}H_{25}N_5O_5S \cdot 0.38C_4H_8O_2$(ethyl acetate)) H, N, S; C: calcd, 56.96; found, 56.13.

5-{[(4S)-4-Hydroxyisoxazolidin-2-yl]carbonyl}-1-isobutyl-3-methyl-6-{[2-(methylamino)-1*H*-benzimidazol-1-yl]methyl}thieno-[2,3-*d*]pyrimidine-2,4(1*H*,3 *H*)-dione (12). Prepared using the same method as for **6** but employing acid **24d** and (*S*)-4-isoxazolidinol hydrochloride[25] (colorless solid, 4.0 g, 58% yield). mp: 232 °C. ^{1}H NMR (300 MHz, DMSO-d_6): δ 7.29−7.17 (m, 2H), 7.00−6.84 (m, 2H), 5.61 (d, $J = 3.8$ Hz, 1H), 5.54−5.17 (m, 2H), 4.85−4.63 (m, 1H), 4.15−3.98 (m, 1H), 3.95−3.52 (m, 5H), 3.21 (s, 3H), 2.96−2.91 (m, 3H), 2.14−1.99 (m, 1H), 0.88−0.81 (m, 6H). APCI-MS *m/z*: (pos) 513 $[M + H]^+$. Anal. ($C_{24}H_{28}N_6O_5S \cdot 1.5H_2O$) C, H, N, S.

(*S*)-6-[(3,5-Dimethyl-1*H*-pyrazol-4-yl)methyl]-5-{[4-hydroxyisoxazolidin-2-yl]carbonyl}-1-isobutyl-3-methylthieno[2,3-*d*]pyrimidine-2,4(1*H*,3*H*)-dione (13). Prepared using the same method as for **6** but employing acid **24** g and (*S*)-4-isoxazolidinol hydrochloride[25] (colorless solid, 2.1 g, 62% yield). mp: 198−202 °C. ^{1}H NMR (300 MHz, DMSO-d_6): δ 12.12 (s, 1H), 5.52 (d, $J = 3.8$ Hz, 1H), 4.79−4.52 (m, 1H), 4.12−3.46 (m, 8H), 3.21 (s, 1H), 3.19 (s, 2H), 2.17−2.00 (m, 7H), 0.87 (d, $J = 6.7$ Hz, 6H). APCI-MS *m/z*: (pos) 462 $[M + H]^+$. Anal. ($C_{25}H_{27}N_5O_5S$) C, H, N, S.

Acknowledgment. The authors thank Y. Whitehead for binding data, B. Stensland for X-ray structure determination, and J. Hackett for assistance with HPLC separations.

Supporting Information Available: Combustion analysis data for compounds **2**−**13**, experimental methods for compounds **16**−**20**, **21c**−**f**, **23**, **24e**−**g**, **26**, **27**, and **29**−**31**, and crystallographic data for compound **8**. This material is available free of charge via the Internet at http:// pubs.acs.org.

References

(1) Michne, W. F.; Schroeder, J. D.; Guiles, J. W.; Treasurywala, A. M.; Weigelt, C. A.; Stansberry, M. F.; McAvoy, E.; Shah, C. R.; Baine, Y.; Sawutz, D. G.; Miller, P. B.; Stankunas, B. M.; Reid, J.; Bump, E.; Schlegel, D. Novel Inhibitors of the Nuclear Factor of Activated T Cells (NFAT)-Mediated Transcription of β-Galactosidase: Potential Immunosuppressive and Antiinflammatory Agents. *J. Med. Chem.* **1995**, *38*, 2557−2569.

(2) Guile, S. D.; Bantick, J. R.; Cheshire, D. R.; Cooper, M. E.; Davis, A. M.; Donald, D. K.; Evans, R.; Eyssade, C.; Ferguson, D. D.; Hill, S.; Hutchinson, R.; Ingall, A. H.; Kingston, L. P.; Martin, I.; Martin, B. P.; Mohammed, R. T.; Murray, C.; Perry, M. W. D.; Reynolds, R. H.; Thorne, P. V.; Wilkinson, D. J.; Withnall, J. Potent Blockers of the Monocarboxylate Transporter MCT1: Novel Immunomodulatory Compounds. *Bioorg. Med. Chem. Lett.* **2006**, *16*, 2260−2265.

(3) Schreiber, S. L. Target-oriented and diversity-oriented organic synthesis in drug discovery. *Science* **2000**, *287*, 1964−1969.

(4) Murray, C. M.; Hutchinson, R.; Bantick, J. R.; Belfield, G. P.; Benjamin, A. D.; Brazma, D.; Bundick, R. V.; Cook, I. D.; Craggs, R. I.; Edwards, S.; Evans, L. R.; Harrison, R.; Holness, E.; Jackson, A. P.; Jackson, C. G.; Kingston, L. P.; Perry, M. W. D.; Ross, A. R. J.; Rugman, P. A.; Sidhu, S. S.; Sullivan, M.; Taylor-Fishwick, D. A.; Walker, P. C.; Whitehead, Y. M.; Wilkinson, D. J.; Wright, A.; Donald, D. K. Monocarboxylate transporter MCT1 is a target for immunosuppression. *Nat. Chem. Biol.* **2005**, *1*, 371−376.

(5) Halestrap, A. P.; Price, N. T. The proton-linked monocarboxylate transporter (MCT) family: structure, function and regulation. *Biochem. J.* **1999**, *343*, 281−299.

(6) Oki, M. Recent advances in atropisomerism. *Top. Stereochem.* **1983**, *14*, 1−81.

(7) Reist, M.; Testa, B.; Carrupt, P.-A.; Jung, M.; Schurig, V. Racemization, Enantiomerization, Diastereomerization and Epimerization: Their meaning and Pharmacological Significance. *Chirality* **1995**, *7*, 396−400.

(8) Friary, R. J.; Spangler, M.; Osterman, R.; Schulman, L.; Schwerdt, J. H. Enantiomerization of an atropisomeric drug. *Chirality* **1996**, *8*, 364−371.

(9) (a) Palani, A.; Shapiro, S.; Clader, J. W.; Greenlee, W. J.; Blythin, D.; Cox, K.; Wagner, N. E.; Strizki, J.; Baroudy, B. M.; Dan, N. Biological evaluation and interconversion studies of rotamers of SCH 351125, an orally bioavailable CCR5 antagonist. *Bioorg. Med. Chem. Lett.* **2003**, *13*, 705−708. (b) Palani, A.; Shapiro, S.; Clader, J. W.; Greenlee, W. J.; Vice, S.; McCombie, S.; Cox, K.; Strizki, J.; Baroudy, B. M. Oximino-piperidino-piperidine-based CCR5 antagonists. Part 2: synthesis, SAR and biological evaluation of symmetrical heteroaryl carboxamides. *Bioorg. Med. Chem. Lett.* **2003**, *13*, 709−712.

(10) (a) Seto, S. Convenient synthesis of 7-aryl-3,4,5,6-tetrahydro-2H-pyrido[4,3-b]- and [2,3-b]-1,5-oxazocine-6-ones. *Tetrahedron Lett.* **2004**, *45*, 8475−8478. (b) Seto, S.; Tanioka, A.; Ikeda, M.; Izawa, S. Design and synthesis of novel 9-substituted-7-aryl-3,4,5,6-tetrahydro-2H-pyrido[4,3-b]- and [2,3-b]-1,5-oxazocin-6-ones as NK1 antagonists. *Bioorg. Med. Chem. Lett.* **2005**, *15*, 1479−1484. (c) Seto, S.; Tanioka, A.; Ikeda, M.; Izawa, S. 2-Substituted-4-aryl-6,7,8,9-tetrahydro-5H-pyrimido[4,5-b][1,5]oxazocin-5-one as a structurally new NK1 antagonist. *Bioorg. Med. Chem. Lett.* **2005**, *15*, 1485−1488.

(11) (a) Ikeura, Y.; Ishichi, Y.; Tanaka, T.; Fujishima, A.; Murabayashi, M.; Kawada, M.; Ishimaru, T.; Kamo, I.; Doi, T.; Natsugari, H. Axially Chiral *N*-Benzyl-*N*,7-dimethyl-5-phenyl-1,7-naphthyridine-6-carboxamide Derivatives as Tachykinin NK1 Receptor Antagonists: Determination of the Absolute Stereochemical Requirements. *J. Med. Chem.* **1998**, *41*, 4232−4239. (b) Natsugari, H.; Ikeura, Y.; Kamo, I.; Ishimaru, T.; Ishichi, Y.; Fujishima, A.; Tanaka, T.; Kasahara, F.; Kawada, M.; Doi, T. Axially chiral 1,7-naphthyridine-6-carboxamide derivatives as orally active tachykinin NK1 receptor antagonists: synthesis, antagonistic activity, and effects on bladder functions. *J. Med. Chem.* **1999**, *42*, 3982−3993. (c) Ishichi, Y.; Ikeura, Y.; Natsugari, H. Amide-based atropisomers in tachykinin NK1-receptor antagonists: synthesis and antagonistic activity of axially chiral N-benzylcarboxamide derivatives of 2,3,4,5-tetrahydro-6H-pyrido[2,3-b][1,5]oxazocin-6-one. *Tetrahedron* **2004**, *60*, 4481−4490.

(12) (a) Albert, J. S.; Aharony, D.; Andisik, D.; Barthlow, H.; Bernstein, P. R.; Bialecki, R. A.; Dedinas, R.; Dembofsky, B. T.; Hill, D.; Kirkland, K.; Koether, G. M.; Kosmider, B. J.; Ohnmacht, C.; Palmer, W.; Potts, W.; Rumsey, W.; Shen, L.; Shenvi, A.; Sherwood, S.; Warwick, P. J.; Russell, K. Design, Synthesis, and SAR of Tachykinin Antagonists: Modulation of Balance in NK1/NK2 Receptor Antagonist Activity. *J. Med. Chem.* **2002**, *45*, 3972−3983. (b) Albert, J. S.; Ohnmacht, C.; Bernstein, P. R.; Rumsey, W. L.; Aharony, D.; Alelyunas, Y.; Russell, D. J.; Potts, W.; Sherwood, S. A.; Shen, L.; Dedinas, R. F.; Palmer, W. E.; Russell, K. Structural Analysis and Optimization of NK1 Receptor Antagonists through Modulation of Atropisomer Interconversion Properties. *J. Med. Chem.* **2004**, *47*, 519−529. (c) Ohnmacht, C. J.; Albert, J. S.; Bernstein, P. R.; Rumsey, W. L.; Masek, B. B.; Dembofsky, B. T.; Koether, G. M.; Andisik, D. W.; Aharony, D. Naphtho[2,1-b][1,5]- and [1,2-f][1,4]oxazocines as selective NK1 antagonists. *Bioorg. Med. Chem.* **2004**, *12*, 2653−2669. (d) Albert, J. S.; Ohnmacht, C.; Bernstein, P. R.; Rumsey, W. L.; Aharony, D.; Masek, B. B.; Dembofsky, B. T.; Koether, G. M.; Potts, W.; Evenden, J. L. Design and optimization of cyclized NK1 antagonists with controlled atropisomeric properties. *Tetrahedron* **2004**, *60*, 4337−4347.

(13) Tucci, F. C.; Hu, T.; Mesleh, M. F.; Bokser, A.; Allsopp, E.; Gross, T. D.; Guo, Z.; Zhu, Y.-F.; Struthers, R. S.; Ling, N.; Chen, C. Atropisomeric property of 1-(2,6-difluorobenzyl)-3-[(2R)-amino-2-phenethyl]-5-(2-fluoro-3- methoxyphenyl)-6-methyluracil. *Chirality* **2005**, *17*, 559−564. and references cited therein.

(14) (a) Corcoran, O.; Spraul, M. LC - NMR - MS in drug discovery. *Drug Discovery Today* **2003**, *8*, 624−631. (b) Silva Elipe, M. V. Advantages and disadvantages of nuclear magnetic resonance spectroscopy as a hyphenated technique. *Anal. Chim. Acta* **2003**, *497*, 1−25.
(15) Abraham, R. J.; Mobli, M.; Smith, R. J. ^{1}H chemical shifts in NMR: part 19. Carbonyl anisotropies and steric effects in aromatic aldehydes and ketones. *Magn. Reson. Chem.* **2003**, *41*, 26−36.
(16) Sternhell, S. Correlation of interproton spin-spin coupling constants with structure. *Q. Rev. Chem. Soc.* **1969**, 236−270.
(17) Johnston, E. R.; Fortt, R.; Barborak, J. C. Correlated rotation in a conformationally restricted amide. *Magn. Reson. Chem.* **2000**, *38*, 932−936.
(18) Clayden, J.; Pink, J. H. Concerted rotation in a tertiary aromatic amide: towards a simple molecular gear. *Angew. Chem., Int. Ed.* **1998**, *37*, 1937−1939.
(19) Bragg, R. A.; Clayden, J.; Morris, G. A.; Pink, J. H. Stereodynamics of bond rotation in tertiary aromatic amides. *Chem. Eur. J.* **2002**, *8*, 1279−1289.
(20) Modelmaker is available from ModelKinetix, Wallingford, United Kingdom, http://www.modelkinetix.com.
(21) Sandström, J. *Dynamic NMR Spectroscopy*;Academic Press: London, 1982; pp 77−92.
(22) Nahm, S.; Weinreb, S. M. N-Methoxy-N-methylamides as effective acylating agents. *Tetrahedron Lett.* **1981**, *22*, 3815−18.
(23) Smallcombe, S. H.; Patt, S. L.; Keifer, P. A. WET solvent suppression and its applications to LC NMR and high-resolution NMR spectroscopy. *J. Magn. Reson.* (Series A) **1995**, *117* 295−303.
(24) Defoin, A.; Pires, J.; Streith, J. Synthesis of aminoerythrose and of aminoerythritol derivatives via Diels-Alder cycloadditions of 1-tert-butyldimethylsiloxybutadiene with acylnitrose dienophiles. *Synlett* **1990**, *2*, 111−13.
(25) Martin, B. P.; Guile, S. D.; Donald, D. K.; Cooper, M. E. A simple and efficient synthesis of optically pure 4-alkylisoxazolidin-4-ols from chiral epoxides. *Tetrahedron Lett.* **2006**, *47*, 7635−7639.

JM060995H